J Electr Eng Technol.2018; 13(3): 1275-1284
http://doi.org/10.5370/JEET.2018.13.3.1275

ISSN(Print) 1975-0102
ISSN(Online) 2093-7423

Comparison of the Characteristics in the Surface Mounted Permanent Magnet and Flux Concentrating Coaxial Magnetic Gears Having the Solid Cores

Ho-Min Shin* and Jung-Hwan Chang†

Abstract – The coaxial magnetic gear with the flux concentrating structure is known that it has the torque performance advantage over the coaxial magnetic gear having surface mounted permanent magnet, thanks to the flux focusing effect. But, if the solid cores are used in the modulating pieces and rotor cores to consider the mechanical reliability and cost reduction, the operating torque of the flux concentrating coaxial magnetic gear can be significantly diminished because the iron losses at the solid cores affect the actual transmitted torque. Furthermore, the modulating pieces and rotor cores have different characteristics of the iron losses from one another, because the space harmonic components of the magnetic flux density, which cause the iron losses, are different. Thus, in this paper, we focused on the analysis of the characteristics of the space harmonic components of the magnetic flux density and resultant eddy current losses in the surface mounted PM and flux concentrating coaxial magnetic gears, when these coaxial magnetic gears have the solid cores at the modulating pieces and rotor cores. The characteristics of pull-out torque (static torque), operating torque (dynamic torque), and efficiency are also researched, and compared by the 3D finite element analysis (FEA) and experiment.

Keywords: Coaxial magnetic gear, Eddy current loss, Flux concentrating rotor, Modulating pieces, Solid core.

1. Introduction

Coaxial magnetic gear (CMG) has the low vibration and noise thanks to the structure of physical isolation between the high-speed rotor and the low-speed rotor, and it can prevent the gear failures like the teeth breaking off in mechanical gear. Furthermore, because there is no reason to lubricate the contact surface periodically, the CMG is advantageous for the reduction of maintenance cost and the realization of clean factory. Due to these advantages, the CMG has been researched as an alternative of mechanical gear in many applications such as wind generation [1-4]. But, to apply the CMG into practical industrial application, we have to consider some important issues for the design of CMG.

Firstly, the mechanical reliability of the fixed part in CMG should be considered. If the modulating pieces are used as the fixed part of CMG, it modulate the magnetic flux produced by permanent magnets (PMs), and at the same time, it also need to withstand the torque corresponding to the sum of torque produced at both rotors. Thus, in case of using the inner and outer part of CMG as the rotor, the modulating pieces, which are placed between the inner and outer part, should function as both the ferromagnetic material to modulate the magnetic flux and the mechanical support to withstand the torque. For this reason, the modulating pieces can be composed of the solid core to improve the stiffness or laminated core to reduce the iron losses. In other words, this selection should be decided by considering the mechanical reliability and the efficiency of CMG, when the designer applies the CMG into the applications.

Secondly, there is an issue about how much the transmitted torque can be improved. As is well known, after the initial model of coaxial structure was suggested by Atallah and Howe, in 2001 [5], the CMG has been researched to increase the maximum transmitted torque [6-11]. In our previous work, we also proposed the flux concentrating (FC) CMG model having torque density of 116 Nm/L, which is 12% bigger than that of CMG with surface mounted PM (SPM) rotor [12]. In case of the CMG model, proposed by K. K. Uppalapati in 2014, the torque density runs to nearly 239 Nm/L [3]. But, it also has the difficulty of manufacturing, because the PM structure of the spoke type is applied at both the inner and outer part. Besides, the modulating pieces are used as the low-speed rotor to improve the maximum transmitted torque, because the gear ratio between the inner part and the modulating pieces is higher than that between the inner part and the outer part. It should be noted that there is a trade-off between the torque improvement and the manufacturing convenience.

Finally, the iron losses, produced at the ferromagnetic

† Corresponding Author: Dept. of Electrical Engineering, Dong-A University, Korea. (cjhwan@dau.ac.kr)
* Dept. of Electrical Engineering, Dong-A University, Korea. (sinhomin@nate.com)
Received: July 18, 2017; Accepted: January 26, 2018

materials in CMG should be investigated. In case of the motor, in general, it is known that the iron loss at the stator, produced by the variation of magnetic flux proportional to the electrical frequency, is much bigger than the iron loss at the rotor core which is produced by the space harmonic component of the magnetic flux density. Similarly, in CMG, the iron loss is largely produced at the modulating pieces due to the periodic variation of the magnetic flux when the modulating pieces are fixed. But, unlike the motor, the CMG, which operated by the flux modulation mechanism, has the considerable iron losses at the rotor core due to the the space harmonic components having the considerable amplitude in the air-gap. Hence, if the solid core is used in the rotor core to consider the cost reduction and the convenience for manufacturing, the characteristics of the iron losses according to the space harmonics of the magnetic flux density should be investigated. Especially, the eddy current loss is largely produced compared with the hysteresis loss because it is proportional to the square of the thickness of the ferromagnetic material. By the same concept, the consideration of the eddy current loss at the modulating pieces is more important compared with the hysteresis loss when the solid core is used in the modulating pieces to improve the stiffness of the fixed part of CMG. Furthermore, at the solid core, the eddy current loss occur largely compared with the PM, because the conductivity of the solid core is four to ten times bigger than that of Neodymium magnet. However, the earlier studies focus on the calculation of eddy current loss at the laminated core, but, the exact cause and amplitude of the eddy current losses according to the space harmonic components of the magnetic flux density have not been reported yet in detail when the solid cores are used in the modulating pieces and rotor cores. Furthermore, though the actual transmitted torque of CMG is significantly decreased proportionally with the iron losses, the characteristics of the operating torque according to the rotating speed have not been mentioned in the previous papers [13-16].

In this paper, we focused on the analysis of the characteristics of the space harmonic components of the magnetic flux density and resultant eddy current losses in the surface mounted PM and flux concentrating coaxial magnetic gears, when these coaxial magnetic gears have the solid cores at the modulating pieces and the rotor cores. The characteristics of pull-out torque (static torque), operating torque (dynamic torque), and efficiency are also researched, and compared by the 3D finite element analysis (FEA) and experiment.

2. Analysis Models of the Coaxial Magnetic Gear

Fig. 1(a) and (b) show the structure of surface mounted PM CMG (SPM CMG) and flux concentrating CMG (FC CMG). The modulating pieces are used as the fixed part of

Table 1. Parameters of the analysis models

	Value
Number of the pole pairs in the inner rotor, p_i	4
Number of the pole pairs in the outer rotor, p_o	22
Number of the modulating pieces	26
Outer diameter [mm]	117
Axial length [mm]	30
Air-gap thickness [mm]	1
PM radial thickness [mm]	6
Remanence of PM [T]	1.25
Core material	SS400
Core conductivity [s/m]	5,882,352

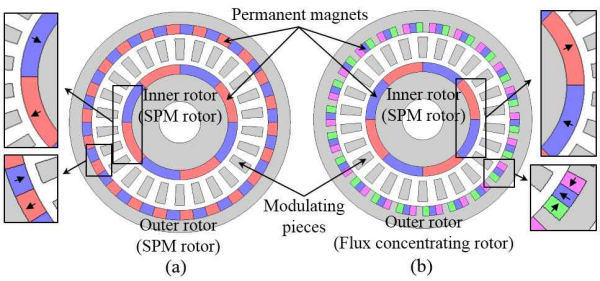

Fig. 1. Structure of the coaxial magnetic gear (CMG): (a) Surface mounted PM coaxial magnetic gear (SPM CMG), (b) Flux concentrating coaxial magnetic gear (FC CMG)

CMG, and the PM rotors are placed in the inner and outer part of CMG. In case of SPM CMG, both the inner rotor and outer rotor has the surface mounted PM structure. But, in case of FC CMG, whereas the inner rotor has the surface mounted PM structure, the outer rotor has the inset PM with flux concentrating structure. In the flux concentrating structure of the outer rotor, the two PM segments adjacent to the left side tooth and right side tooth are tangentially magnetized toward the center of slot, and the PM placed in the center of slot is radially magnetized toward the air-gap. In both the SPM CMG and FC CMG, the solid cores with steel, SS400, are used in the modulating pieces and rotor cores to consider the mechanical reliability, cost reduction and convenience for manufacturing. The parameters and specifications are presented in table 1.

The magnetic field produced by PMs are modulated by the modulating pieces and synchronized with the magnetic field produced by PMs of the opposite side rotor. In other words, in the inner air-gap, the magnetic field produced by the inner PM is synchronized with the modulated magnetic field produced by the outer PM, and in the outer air-gap, the magnetic field produced by the outer PM is synchronized with the modulated magnetic field produced by the inner PM. By this modulation effect, the inner rotor, which has a 4 pole pairs, rotates with the high speed, and the outer rotor, which has a 22 pole pairs, rotates with the low speed. Therefore, the gear ratio with two rotors can be expressed as -5.5 (= -22/4) by the number of pole pairs of each rotor [5]. In this gear ratio, the minus sign means

that the two rotors rotate in the opposite direction to each other.

3. Analysis of Torque Characteristics

Fig. 2 shows the design variables for the optimization using the response surface methodology in the FC CMG. The width ratios with respect to the non-magnetized area in the inner magnet, air region between the modulating pieces, radial magnetized PM in the outer magnet, and tooth in the outer rotor are defined as x_1, x_2, x_3 *and* x_4, respectively. The optimization process is presented in [12], and the optimum sets of width ratios of the non-magnetized area in the inner magnet and the air region between the modulating pieces are identically applied in SPM CMG.

Table 2 shows the pull-out torque calculated by FEA in SPM CMG and FC CMG. In case of FC CMG, due to the concentrating effect of the flux toward the air-gap, the working harmonic, which contributes to the torque production, is increased. For this reason, in results of 2D FEA, the pull-out torque of FC CMG is improved by more than 12% compared with that of the SPM CMG. But, in 3D FEA, the pull-out torque of FC CMG, which are calculated at the outer rotor, is only increased by 7.6%. This is because of the fact that the axial flux leakage at the flux concentrating rotor in FC CMG is severe compared with that of the rotor in SPM CMG. The torque ratio of 3D result to 2D result in FC CMG is 73.5%, and it is lower than 76.1% of SPM CMG. But, it should be noted that the results of the pull-out torque, which ignore the influence of the transmitted torque reduction by the eddy current losses, will be different with the results of the operating torque. This characteristic will be presented in the next chapters, 4 and 5.

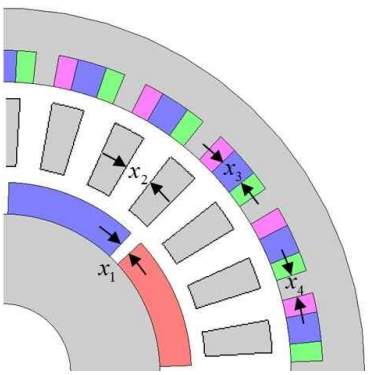

Fig. 2. Design variables for optimization

Table 2. Comparison of the pull-out torque characteristics

Content		2D FEA		3D FEA	
		SPM CMG	FC CMG	SPM CMG	FC CMG
Torque (N.m)	Inner rotor	6.09 (100%)	6.79 (112%)	4.65 (100%)	5.06 (108.8%)
	Outer rotor	33.48 (100%)	37.33 (112%)	25.49 (100%)	27.43 (107.6%)
Torque/Volume (kN.m/m^3)		103.8 (100%)	115.7 (112%)	79 (100%)	85.1 (107.6%)
Torque/PM Volume (kN.m/m^3)		340.2 (100%)	465.8 (137%)	259 (100%)	342.3 (132.2%)
3D/2D Torque ratio		·	·	76.1%	73.5%

4. Eddy Current Losses at the Solid Cores

CMG has no friction loss due to the contactless structure. Moreover, since the CMG does not have the current source, the iron loss is only considered in the electrical losses when the CMG is designed. But, in case of using the solid core, the eddy current loss, which are proportional to the square of the thickness of the ferromagnetic materials, are largely produced compared with the hysteresis loss. In addition, although the magnetic flux, produced by the PM, passes through the modulating pieces, there are some space harmonic components of flux density which are not synchronized with the PM rotor. Thus, we have to analyze not only the amplitude of the eddy current losses at each solid core of CMG but also the detailed causes in terms of the space harmonic components of magnetic flux density.

Fig. 3(a) and (b) show the 3D FEA results of the eddy current losses at solid cores with the speed variation in

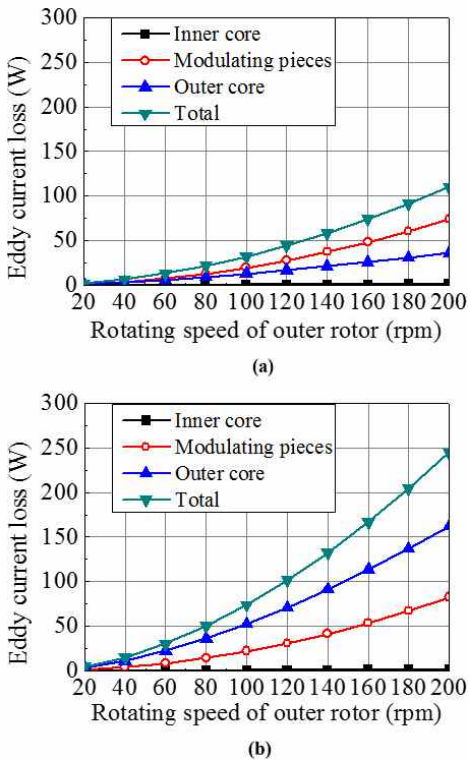

Fig. 3. Eddy current losses at the ferromagnetic materials with the speed variation in the condition of the no-load: (a) Surface mounted PM coaxial magnetic gear (SPM CMG), (b) Flux concentrating coaxial magnetic gear (FC CMG)

SPM CMG and FC CMG when the two rotors have the no-load condition. It should be noted that the analysis model of CMG in FEA, to calculate the eddy current loss, should be designed considering the skin effect. Thus, the FEA models have the fine mesh at each solid core. The total eddy current losses at solid cores are considerably increased in both CMG models as the rotor speed rises, because the eddy current loss are directly proportional to the square of the electrical frequency of the magnetic flux. However, the eddy current loss is rarely produced at the inner core in both CMG models regardless of variation of rotor speed, and the eddy current losses at the modulating pieces in SPM CMG and FC CMG are similar to each other. On the other hand, the eddy current losses at the outer core in FC CMG are almost four times bigger than those of SPM CMG. Besides, they are also bigger than those at the modulating pieces. As shown in Fig. 4, we can see that the saturation at the tip of the outer core in FC CMG has influence on the eddy current losses. But, the saturation cannot be regarded as the only cause for the generation of the large eddy current losses at the outer core. Namely, the eddy current losses at the outer core can be thought of as the phenomenon caused by the space harmonic components of the flux density at the air-gap. Thus, to understand the results in rotor cores more of the no-load: (a) Surface mounted PM coaxial magnetic gear (SPM CMG), (b) Flux concentrating coaxial magnetic gear (FC CMG) clearly, the characteristics of the space harmonic components of flux density at the air-gap should be presented, and they need to be separately analyzed in terms of the components which cause the eddy current losses at the inner core and the outer core.

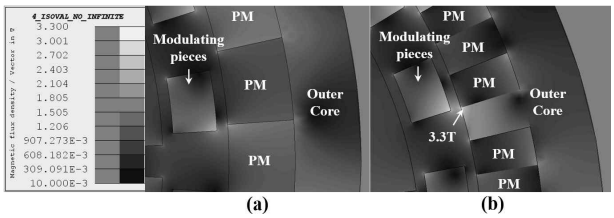

Fig. 4. Magnetic flux density distribution with the condition

Using the analysis of superposition, we can separate the magnetic source of CMG. Fig. 5 shows the analysis model with the inner PM excitation and its space harmonic spectra of flux density at the air-gap. As shown in Fig. 5(a), the PMs of the outer rotor are replaced with the air region. Fig. 5(b) and (c) show the space harmonic spectra of the flux density at the inner air-gap and the outer air-gap adjacent to the modulating pieces, respectively. In the inner air-gap, understandably, the 4th space harmonic component corresponding to the pole pair of inner PM, p_i is dominantly produced, and in the outer air-gap, the 22nd space harmonic component corresponding with the pole pair of outer PM, p_o is produced by the modulation effect. But, in case of the outer air-gap, it should be noted that there is the 4th space harmonic component which has the bigger amplitude than the 22nd space harmonic component corresponding to the working harmonic. This 4th space harmonic component rotates at the same speed with the inner rotor. It means that the unmodulated harmonic components can be produced at the other side of the air-gap even though the magnetic field passes through the modulating pieces. In addition, this unmodulated 4th space harmonic component at the outer air-gap flows through the outer core as shown in Fig. 5(d). But, the other space harmonic components, which include the modulated and unmodulated space harmonic components, have negligible amplitude at the outer core. Thus, we can infer that the unmodulated 4th space harmonic component is the main cause of the eddy current loss at the outer core.

The unmodulated space harmonic component at the outer air-gap by the inner PM excitation rotates at the same speed with the inner rotor regardless of its order, and it moves with the opposition direction to the outer rotor. Thus, from the viewpoint of the outer core, the rotating speed of the unmodulated space harmonic component, which is produced by the inner PM excitation, can be derived by the summation of the rotating speed of both rotors, and the frequency of eddy current loss caused by this unmodulated space harmonic component at the outer core can be expressed as follows.

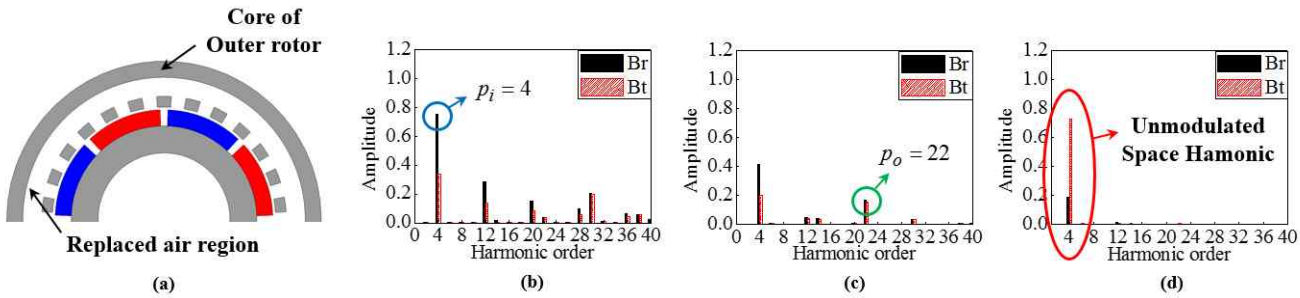

Fig. 5. Space harmonic analysis by inner PM excitation in SPM CMG: (a) Analysis model of the inner PM excitation in which the PM of outer rotor is replaced with the air region, (b) Harmonic spectra of flux density at the center of the inner air-gap, (c) Harmonic spectra of flux density at the outer air-gap adjacent to the modulating pieces, (d) Harmonic spectra of flux density at the outer core

$$f_{eddy} = Q_i \cdot \frac{(n_i + n_o)}{60}[Hz] \quad (1)$$

where, the n_i and n_o are the revolutions per minute of inner rotor and outer rotor, respectively, and Q_i is the space harmonic order.

Next, Fig. 6 shows the analysis model with the outer PM excitation and its space harmonic spectra of flux density at the air-gap. In case of the outer PM excitation, the PMs of inner rotor are replaced with the air region as shown in Fig. 6(a). Fig. 6(b) and (c) show the space harmonic spectra of the flux density at the inner air-gap adjacent to the modulating pieces and the outer air-gap, respectively. In case of the outer air-gap, the 22nd space harmonic component is dominantly produced, and in the case of inner air-gap, the 4th space harmonic component corresponding to the pole pair of inner PM is produced by the modulation effect. Besides, similar to the characteristics of the modulation in the inner PM excitation, the unmodulated 22nd space harmonic component exists in the inner air-gap although it passes through the modulating pieces. But, in this case, the unmodulated 22nd space harmonic component at the inner air-gap does not flow through the inner core. In other words, it only passes through the modulating pieces

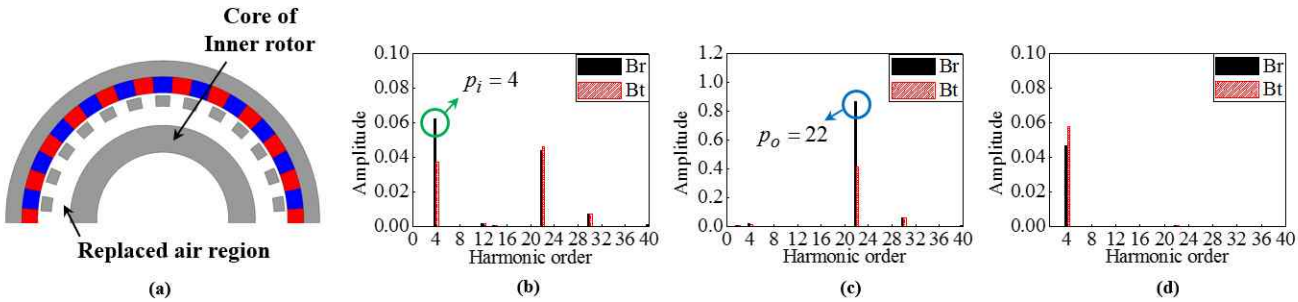

Fig. 6. Space harmonic analysis by outer PM excitation in SPM CMG: (a) Analysis model of the outer PM excitation in which the PM of inner rotor is replaced with the air region, (b) Harmonic spectra of flux density at the inner air-gap adjacent to the modulating pieces, (c) Harmonic spectra of flux density at the center of the outer air-gap, (d) Harmonic spectra of flux density at the inner core

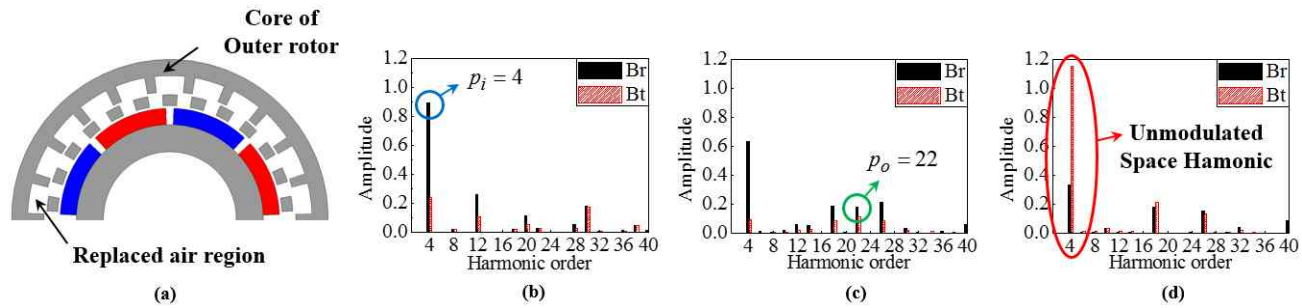

Fig. 7. Space harmonic analysis by inner PM excitation in FC CMG: (a) Analysis model of the inner PM excitation in which the PM of outer rotor is replaced with the air region, (b) Harmonic spectra of flux density at the center of the inner air-gap, (c) Harmonic spectra of flux density at the outer air-gap adjacent to the modulating pieces, (d) Harmonic spectra of flux density at the outer core

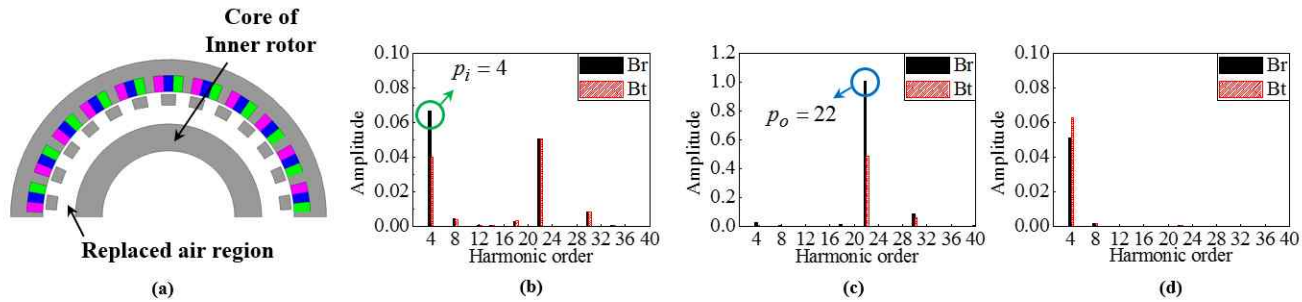

Fig. 8. Space harmonic analysis by outer PM excitation in FC CMG: (a) Analysis model of the outer PM excitation in which the PM of inner rotor is replaced with the air region, (b) Harmonic spectra of flux density at the inner air-gap adjacent to the modulating pieces, (c) Harmonic spectra of flux density at the center of the outer air-gap, (d) Harmonic spectra of flux density at the inner core

because the length of the effective air-gap in the inner part is long compared with the pole pitch of outer PM. Hence, as shown in Fig. 6(d), the unmodulated 22nd space harmonic component is not produced at the inner core, and

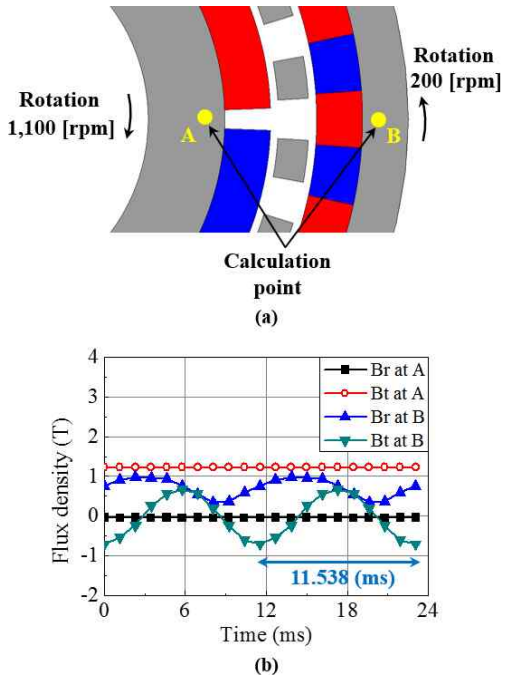

Fig. 9. Radial and tangential flux density variations at cores of both rotors in SPM CMG: (a) Calculation points, (b) Wave forms according to the time

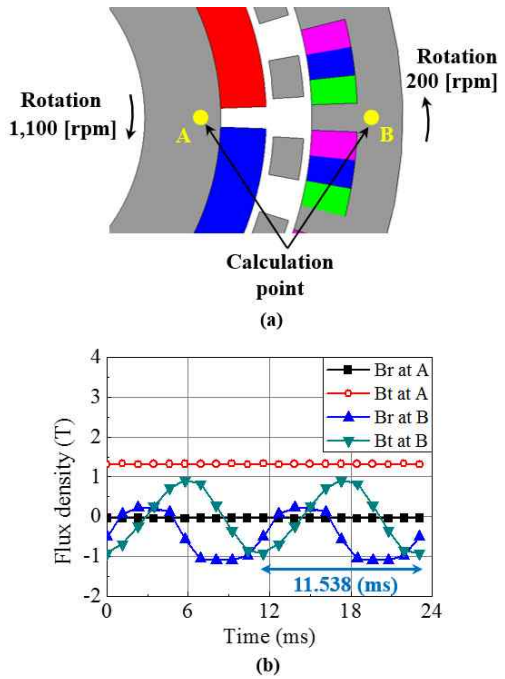

Fig. 10. Radial and tangential lux density variations at cores of both rotors in FC CMG: (a) Calculation points, (b) Wave forms according to the time

the PMs of the outer rotor have no significant influence on the eddy current losses at the inner core. By the above two analysis cases, we can think that the characteristic difference of the eddy current losses at the inner core and outer core is derived by the unmodulated space harmonic component of flux density.

Fig. 7 and Fig. 8 show the analysis models with the inner PM excitation and the outer PM excitation in FC CMG. The characteristics of the magnetic field modulation are similar to those of SPM CMG, but the unmodulated 4th space harmonic component at the outer core, produced by the inner PM, has the large amplitude compared to that of SPM CMG as shown in Fig. 5(d) and Fig. 7(d). It is because the FC CMG with the inset type core has much shorter effective air-gap compared with that of SPM CMG. As a result, this unmodulated 4th space harmonic component causes the large eddy current losses at the outer core in FC CMG as shown in Fig. 3(b). Fig. 9(a) and Fig. 10(a) show the calculation points, A and B, of flux densities, and these calculation points rotate with each rotor core. Also, Fig. 9(b) and Fig. 10(b) show the variations of the radial and tangential magnetic flux densities at the rotor cores in SPM CMG and FC CMG, when the inner rotor and the outer rotor rotate at 1,100rpm and 200rpm, respectively. In both CMG models, the flux densities at the inner core are hardly varied regardless of the rotation. But, in case of the outer core, we can see that the variations of the flux densities have the frequency, 86.67 Hz (=1/11.538 ms), and it is equal to the frequency calculated by (1). Furthermore, in FC CMG, the amplitudes of the radial and tangential flux density waveform are bigger than those of the SPM CMG. This is because the unmodulated space harmonic at the outer core in FC CMG is larger than that of the SPM CMG at point B.

5. Experimental Evaluation

As mentioned above, the eddy current losses have large influence in the torque characteristics, and it will cause the reduction of the actual transmitted torque. Particularly, as shown in section 4, when the CMG has the solid cores, the eddy current losses by the unmodulated space harmonic component of flux density are quite large. Thus, when the CMG rotates, the actual transmitted torque according to the speed variation is important. To evaluate these torque characteristics, the dynamometer tests are carried out in the prototype of SPM CMG and FC CMG.

Fig. 11 shows the dynamometer used in the torque characteristics test of SPM CMG and FC CMG. The servo motor and the powder brake are connected to the input and output of CMG, respectively. Fig. 12 shows the assembly view of CMG, and Fig. 13 shows the components of the prototype, namely, two rotors, four bearings, modulating part, and housings. The manufacturing of CMG is difficult because it has the complex structure which consists of

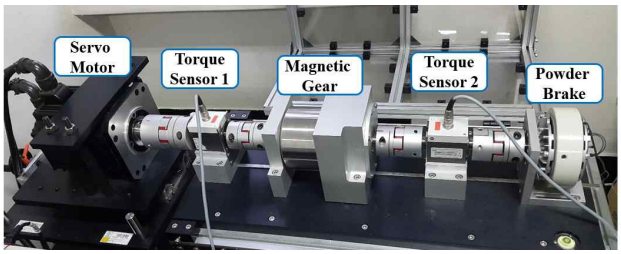

Fig. 11. Dynamometer for the torque characteristics test of CMG

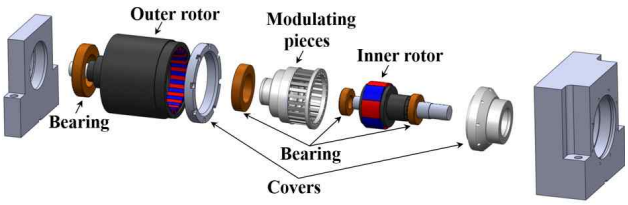

Fig. 12. Assembly view of CMG

Fig. 13. Component of the prototype of CMG: (a) Modulating pieces (Fixed part), (b) Surface mounted PM and outer core in SPM CMG, (c) Flux concentrating PM and outer core in FC CMG, (d) Surface mounted PM, inner core and inner shaft in SPM CMG and FC CMG

two rotation parts and one fixed part. Furthermore, in the fixed part of CMG, the modulating pieces suffer from the periodical vibration due to the radial force produced by the magnetic flux, and they also need to withstand the torque corresponding to the sum of torque produced at both rotors. Hence, each modulating piece of prototypes is bolted to its cover. But, the holes at each modulating piece did not have effect on the results of the torque analysis in 3D FEA, because these holes are placed in the axial flux leakage region.

Fig. 14 shows the comparison of the pull-out torque between the 3D FEA and the experiment in SPM CMG and FC CMG. To get the pull-out torque, the inner rotor is fixed by the powder brake, and the outer rotor is rotated by the servo motor. The experiment results of the pull-out torque are almost the same as those of 3D FEA in SPM CMG and FC CMG. But, it should be noted that the pull-out torque in the static condition is of little importance, because it will be reduced by the eddy current losses at the solid cores when the CMG rotates. Thus, the dynamic tests of the CMG are also performed.

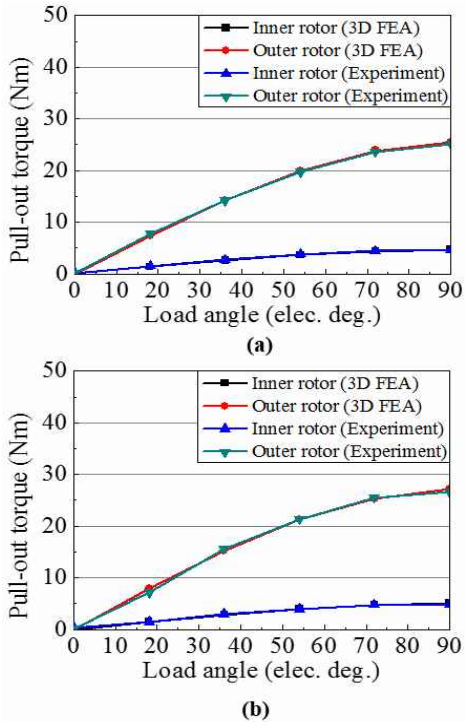

Fig. 14. Comparison of pull-out torque between 3D FEA and experiment: (a) Surface mounted PM coaxial magnetic gear (SPM CMG), (b) Flux concentrating coaxial magnetic gear (FC CMG)

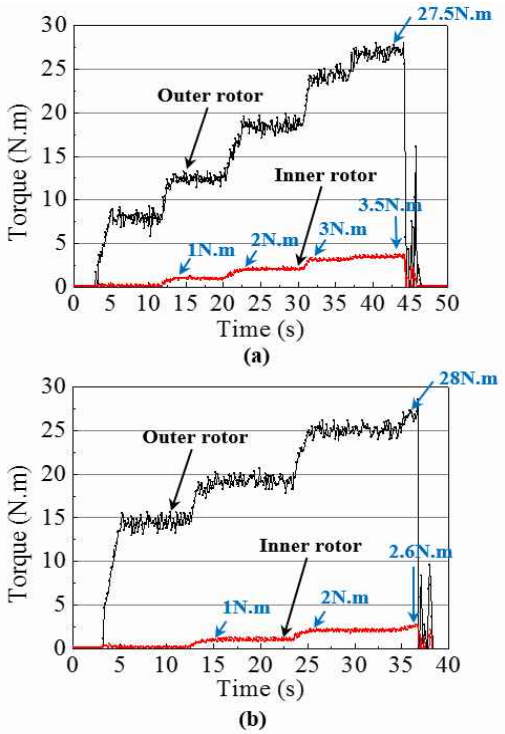

Fig. 15. Characteristics of actual transmitted torque with load variation when the CMG rotates at 1,100rpm and 200rpm in the inner rotor and outer rotor, respectively: (a) Surface mounted PM coaxial magnetic gear (SPM CMG), (b) Flux concentrating coaxial magnetic gear (FC CMG)

Fig. 15 shows the characteristics of actual transmitted torque with the load variation in SPM CMG and FC CMG when the CMG rotates at 1,100rpm and 200rpm in the inner rotor and outer rotor, respectively. Until the pulling out of step (loss of synchronism) between the inner rotor and outer rotor occurs, the rotors keep the gear ratio between each other. However, when the load torque is bigger than the actual transmitted torque, the pulling out of step happens, and this phenomenon continues for some time. During the hunting of CMG, the fixed part, which includes the modulating pieces, undergoes considerable vibration due to the magnetic torque with the alternating direction in a very short time. This phenomenon is the problem which must be solved to apply the CMG in the practical industrial application. Furthermore, the reduction of the actual transmitted torque by the eddy current losses also clearly appeared. In case of SPM CMG, the inner rotor, which is the output, can be subjected to the torque up to the maximum 3.5Nm as shown in Fig. 15(a). But, the calculated input torque multiplied by the gear ratio, 5.5, is only 19.25Nm, and it is about 71% of the actual input torque, 27.5Nm. It means that the torque difference between the calculated input torque and the actual input torque is the loss corresponding to the eddy current losses and the mechanical losses. In case of FC CMG, as we might expect, this torque difference between the calculated input torque and the actual input torque is bigger than that of SPM CMG due to the large eddy current losses. As shown in Fig. 15(b), the inner rotor of FC CMG can be subjected to the torque up to the maximum 2.6Nm. However, the calculated input torque multiplied by the gear ratio, 5.5 is only 14.3Nm, which is about 51% of the actual input torque, 28Nm. It should be noted that the actual transmitted torque of FC CMG, 14.3Nm is even smaller than 19.25Nm which is actual transmitted torque of SPM CMG, because of the large eddy current losses at the outer core. To estimate the transmitted torque loss according to the speed variation, the no-load losses in SPM CMG and FC CMG are presented together with the FEA results as shown in Fig. 16. The experiment results of the no-load losses in FC CMG are bigger than those of the SPM CMG, and it may be caused by the large eddy current losses at the outer core. As a results of the no-load losses, the difference between the results of FEA and experiment can be considered as the mechanical losses at four bearings, hysteresis losses at the solid cores, iron losses at PM, and the extra mechanical losses, because the FEA results of no-load losses are only the eddy current losses at the solid cores.

Fig. 17 shows the experiment results of the efficiency with speed variation according to load in SPM CMG and FC CMG. In both CMG models, the efficiencies are considerably decreased by the eddy current losses as the CMG rotates faster, and, specially, the efficiencies of FC CMG are lower than those of SPM CMG due to the large eddy current losses. Furthermore, in case of FC CMG, the pulling out of step between the inner and the outer rotor occurs after the inner rotor rotates at higher speed than 660rpm when the load torque is 3Nm.

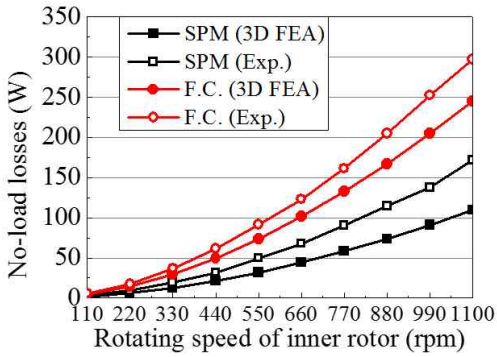

Fig. 16. Comparison of no-load losses with speed variation between 3D FEA and experiment in SPM CMG and FC CMG

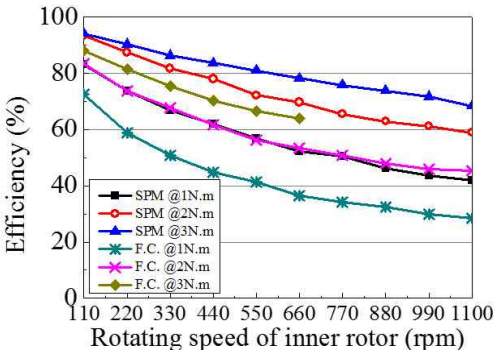

Fig. 17. Comparison of the efficiencies with speed variation according to load in SPM CMG and FC CMG

6. Conclusion

The CMG with the surface mounted PM rotor and the flux concentrating rotor are evaluated in terms of the eddy current losses, static torque, dynamic torque, and efficiencies, when the solid cores are used in the modulating pieces and the rotor cores. In both models, the unmodulated 4th space harmonic component which is not synchronized with the outer rotor is produced at the outer air-gap, and it causes the large eddy current losses at the outer core. Specially, the eddy current loss at the outer core in FC CMG is largely produced because of the large unmodulated space harmonic component of flux density. In case of SPM CMG, the eddy current loss at the modulating pieces by the periodic variation of the magnetic flux is larger than that of outer core. On the other hand, in both models, the unmodulated space harmonics at the inner air-gap by the outer PM have no significant influence on the eddy current losses at the inner core because the length of

the effective air-gap in the inner part is too long compared with the pole pitch of the outer PM. Thus, in high-speed application, the outer core rather than the inner core in CMG needs to be laminated to reduce the eddy current loss produced by the unmodulated space harmonic. Finally, because the actual transmitted torque and the efficiencies are decreased proportionally with the eddy current losses, the characteristics of the CMG should be investigated according to the speed.

Acknowledgements

This work was supported by the Korea Institute of Energy Technology Evaluation and Planning (KETEP) and the Ministry of Trade, the Industry and Energy (MOTIE) of the Republic of Korea (no. 20152020000750); and the Basic Science Research Program through the National Research Foundation (NRF) of Korea funded by the Ministry of Education (NRF-2015R1D1A1A01059637).

References

[1] L. Shah, A. Cruden, and B. W. Williams, "A magnetic gear box for application with a contra-rotating tidal turbine," *in Proc. of PEDS*, pp. 989-993, Apr. 2007.

[2] K. K. Uppalapati, J. Z. Bird, D. Jia, J. Garner, and A. Zhou, "Performance of a magnetic gear using ferrite magnets for low speed ocean power generation," *in Proc. of ECCE*, pp. 3348-3355, Nov. 2012.

[3] K. K. Uppalapati, J. Z. Bird, J. Wright, J. Pitchard, M. Calvin, and W. Williams "A magnetic gearbox with an active region torque density of 239Nm/L," *in Proc. of ECCE*, pp. 1422-1428, Sept. 2014.

[4] K. K. Uppalapati, J. Z. Bird, and J. Wright, "Experimental evaluation of low-speed flux-focusing magnetic gearboxes," *IEEE Trans. Ind. Appl*., vol. 50, no. 6, pp. 3637-3643, Mar. 2014.

[5] K. Atallatuh, S. D. Calverley, and D. Howe "Design, analysis and realization of a high-performance magnetic gear," *IEE Proc. of Electr. Power Appl*., vol. 151, no. 2, pp. 135-143, Mar. 2004.

[6] P. O. Rasmussen, T. O. Andersen, F.T. Joergensen, and O. Nielsen "Development of a high performance magnetic gear," *IEEE Trans. Ind. Appl*., vol. 41, no. 3, pp. 764-770, May. 2005.

[7] X. Li, K. T. Chau, M. Cheng, W. Hua, and Y. Du, "An improved coaxial magnetic gear using flux focusing," *in Proc. of ICEMS*, Aug. 2011.

[8] K. Uppalapati and J. Bird "A flux focusing ferrite magnetic gear," *in Proc. of PEMD*, Mar. 2012.

[9] X. Li, K. T. Chau, M. Cheng, W. Hua, and Y. Du, "A new coaxial magnetic gear using stationary permanent magnet ring," *in Proc. of ICEMS*, pp. 634-638, Oct. 2013.

[10] S. Peng, W. N. Fu, and S. L. Ho, "A novel high torque-density triple-permanent-magnet-excited magnetic gear," *IEEE Trans. Magn*., vol. 50, no. 11, Nov. 2014.

[11] Y. Chen, W. N. Fu, and W. Li, "Performance analysis of a novel triple-permanent-magnet-excited magnetic gear and its design method," *IEEE Trans. Magn*., vol. 52, no. 7, Jul. 2016.

[12] H. M. Shin and J. H. Chang, "Design of coaxial magnetic gear for improvement of torque characteristics," *KMS Journal of magnetics*, vol. 19, no. 4, pp. 393-398, Dec. 2014.

[13] L. Jian, K. T. Chau, Y. Gong, J. Z. Jiang, C. Yu, and W. Li, "Comparison of coaxial magnetic gears with different topologies," *IEEE Trans. Magn*., vol. 45, no. 10, pp. 4526-4529, Oct. 2009.

[14] M. Fukuoka, K. Nakamura, and O. Ichinokura, "Loss analysis and performance improvement of trial SPM type magnetic gear," *in Proc. of EPE*, Sept. 2013.

[15] K. Nakamura, M. Fukuoka, and O. Ichinokura, "Performance improvement of magnetic gear and efficiency comparison with conventional mechanical gear," *J. Appl. Phys*., vol. 115, no. 17, Apr. 2014.

[16] M. Johnson, A. Shapoury, P. Boghrat, M. Post, and H. A. Toliyat, "Analysis and development of an axial flux magnetic gear," *in Proc. of ECCE*, pp. 5893-5900, Sept. 2014.

Homin Shin received B.S. and M.S. degrees in Electrical Engineering from Department of Electrical Engineering, Dong-A University, Busan, Republic of Korea in 2016. He is currently pursuing the Ph.D. degree in Motor Design and control from Mechatronics System Research Laboratory, Depart-ment of Electrical Engineering, Dong-A University. His research interests include motor design & drive such as synchronous motor, induction motor and magnetic geared motor, and design of electro -mechanical systems such as electrically driven machine tools and magnetic gear. Homin Shin is a graduate student member at the Institution of Engineering and Technology, U.K, Institute of Electrical and Electronics Engineers, USA, Institute of Electrical Engineers, Repulic of Korea.

Junghwan Chang received B.S. and M.S. degrees in electrical engineering and Ph.D. degree in precision mechanical engineering from Hanyang University, Seoul, Republic of Korea in 1994, 1997 and 2001, respectively. From 2001 to 2002, he worked at Institute of Brain Korea 21 at Hanyang

University, where he developed micro drive and high - speed spindle motor. From 2002 to 2003, he worked as research fellow at University of California at Berkeley with the support of Korea Science and Engineering Foundation, and analyzed and developed electrically controlled engine valve system. From 2003 to 2009, he worked in Korea Electrotechnology Research Institute (KERI) as a technical leader, and engaged in the developments of special purpose machines. Since 2009, he has been with the department of electrical engineering, Donga University, Busan Rep. of Korea, as an associate professor. His interests are the design and analysis of electro -mechanical systems such as electrically driven machine tools and magnetic gear.
Prof. Chang is a member of Institute of Electrical and Electronics Engineers, USA and Korea Institute of Electrical Engineers, Republic of Korea. He works as a reviewer for *IEEE TRANSACTION ON MAGNETICS*, *IEEE TRANSACTION ON INDUSTRIAL APPLICATION*, *IEEE TRANSACTION ON INDUSTRIAL ELECTRONICS AND IEEE TRANSACTION ON SUPERCONDUCTIVITY*. He worked as steering committee member and Technical Program Chair in different conferences likes IEEE ITEC Asia - Pacific 2016, ICEMS 20 13 etc.